

RESEARCH

Open Access



Mechanical Behavior of Recycled Fine Aggregate Concrete with High Slump Property in Normal- and High-Strength

Minkwan Ju¹, Kyoungsoo Park^{1*} and Won-Jun Park²

Abstract

This study investigated the mechanical behavior of normal strength (NS) and high strength (HS) concrete containing recycled fine aggregates (RFAs). A high slump mixing design was employed, which may be potentially used as filled structural concrete. The compressive strength, tensile strength, and elastic modulus were measured according to the RFA replacement ratio and curing time. In addition, the shrinkage strain was measured in a temperature and humidity chamber over 260 days. The compressive strength and elastic modulus of RFA concrete were approximately 70–90% of those of virgin concrete. The decreases in the compressive strength and elastic modulus for NS concrete were larger than those for HS concrete. This could be explained by the difference in failure mechanism between NS and HS concrete. The average ratio of the compressive strength at 190 days to that at 28 days was 1.15–1.3, and the ratio of the tensile strength at 190 days to that at 28 days was 1.15–1.25. These demonstrate good strength development. The ratios between the elastic modulus and compressive strength for RFA concrete were dissimilar to those for virgin concrete but similar to those for recycled coarse aggregate concrete. ACI318-14 (Building code requirements for structural concrete and commentary, 2014) and Model Code (Fibmodel code for concrete structures, 2010) overestimated the elastic modulus of RFA concrete. Therefore, this study suggested an empirical expression to approximate the elastic modulus of RFA concrete. The increase in shrinkage owing to the use of RFA was at most 5–6% of the ultimate compressive strain of concrete.

Keywords: recycled fine aggregate, normal- and high-strength concrete, high slump, compressive and tensile strength, elastic modulus

1 Introduction

The construction industry is responsible for 50% of the consumption of natural resources. The importance of recycling construction materials has been emphasized owing to the depletion of natural resources. A strategy to overcome the supply shortage of natural aggregates is the partial (or full) use of coarse and fine recycled aggregates (RAs). To utilize RA concrete as a structural concrete member, its mechanical behaviors should be investigated comprehensively. The use of recycled coarse aggregates

(RCA) has been investigated extensively, including the use of structural concrete member (McNeil and Kang 2013; Sagoe-Crentsil et al. 2001; Smith et al. 2014; Wang et al. 2016; Wardeh et al. 2015), recycling ceramic waste (Alves et al. 2014; Zegardło et al. 2018) and the surface modification effects of RCA (Choi et al. 2016; Ryou and Lee 2014; Ryu et al. 2018).

Previous studies revealed that for a normal strength range, the compressive strength of RCA concrete decreased by approximately 15–30% from that of natural aggregate (NA) concrete as the RCA replacement ratio increased to 100% (Folino and Xargay 2014; McNeil and Kang 2013). A current study has reported that the decrease in the compressive strength was less than 10% (Knaack and Kurama 2014; Tahar et al. 2017; Xie and Ozbakkaloglu 2016). For a high strength range of over

*Correspondence: k-park@yonsei.ac.kr

¹ Department of Civil and Environmental Engineering, Yonsei University, Seoul, Republic of Korea

Full list of author information is available at the end of the article
Journal information: ISSN 1976-0485 / eISSN 2234-1315

55 MPa and 100% replacement with RCA, the compressive strength of RCA concrete was approximately 10% less than that of virgin concrete (Kanellopoulos et al. 2014; Pedro et al. 2017; Tam et al. 2015; Xie and Ozbakkaloglu 2016). Recent studies on RCA concrete have reported that high strength (HS) concrete with RCA did not exhibit a significant reduction in the compressive strength. Furthermore, other mechanical properties such as the elastic modulus, indirect tensile strength, flexural strength, toughness, and fracture energy for RCA concrete were evaluated (Gholampour and Ozbakkaloglu 2018; Kou and Poon 2008; Zhou and Chen 2017). In addition, the time dependent behaviors were investigated by measuring the shrinkage and creep strains according to the RCA replacement ratio (Seo and Lee 2015; Tam et al. 2015).

However, relatively few studies on recycled fine aggregates (RFAs) concrete have been performed because of the high porosity and high water absorption for RFA. The relatively high porosity of old cement paste leads to poor characteristics of the interfacial transition zone (ITZ) (Gómez-Soberón 2002). Because of the high porosity of RFA, an water absorption rate of RFA was 11–13% (Evangelista and Brito 2007; Katz 2003; Kumar et al. 2017; Pereira et al. 2012a, b), which was higher than that of natural fine aggregate. High water absorption can reduce the workability during concrete mixing. Moreover, drying shrinkage strain can increase with an increase in the replacement ratio of RFA.

Recently, the mechanical behaviors of RFA concrete have been enhanced. For RFA concrete with 100% replacement ratio, for example, Kumar et al. (2017) reported that the reductions in the compressive and splitting tensile strengths were 16% and 7.0%, respectively. For high strength concrete with RFA, the reduction in the compressive strength was 4–12% and the reduction in the splitting tensile strength was 24% for 100% RFA concrete (Pedro et al. 2017; Pereira et al. 2012a, b; Santos et al. 2017). Additionally, most measured slump values of previous RFA concrete (Kurda et al. 2017; Pedro et al. 2017; Pereira et al. 2012a, b) were in the range of 80–134 mm. Although Yang et al. (2008) utilized high slump RFA concrete, i.e., 175–200 mm, their investigation was limited to the normal strength RFA concrete.

However, in comparison to studies on RCA concrete, those on RFA concrete are still scant, particularly for its use as a structural concrete member. Thus, further comprehensive investigations on the mechanical behaviors of RFA concrete with high slump property are required, including those that study enhancements to NS and HS concrete with pozzolanic powder, various replacement ratios of RFA up to 100%, and long-term behaviors of these mixtures.

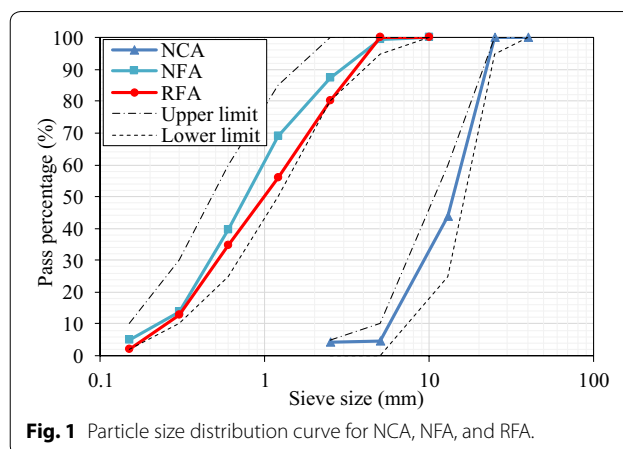


Fig. 1 Particle size distribution curve for NCA, NFA, and RFA.

In this study, the mechanical behaviors of NS and HS concrete mixed with RFA were evaluated according to the RFA replacement ratio and curing time. These behaviors included the compressive strength, indirect tensile strength, elastic modulus, and shrinkage strain. Five RFA replacement ratios were employed for both NS and HS concrete with the average slump of 214 and 217 mm, respectively. The compressive strength was measured at 3, 7, 28, and 190 days, whereas the splitting tensile strength was measured at 28 and 190 days. The long-term behavior was evaluated by measuring the drying shrinkage strain until 260 days. The measured compressive modulus of elasticity was compared with the previous experimental data on RFA and RCA concrete. Moreover, an empirical expression to predict the elastic modulus of RFA concrete is suggested.

2 Experimental Program

NS and HS mixing designs with five replacement ratios of RFA were used to investigate mechanical behavior. The compressive strength, splitting tensile strength, and modulus of elasticity were evaluated. In addition, the drying shrinkage strain was measured for investigating the long-term behavior.

2.1 Materials

Three types of aggregates were utilized in this study: natural coarse aggregate (NCA), natural fine aggregate (NFA), and RFA. NCA was prepared by crushing natural gravel, and NFA was obtained from river sand. RFA was obtained from a domestic manufacturer with a quality certification for producing recycled concrete aggregate (Sim and Won 2010; Won 2006; Won and Sim 2009). NFA and RFA were prepared from saturated surface dried (SSD) condition using ASTM C128 (2015). The grain size distribution curves of the three aggregates are shown in Fig. 1. The curves present that the aggregates

Table 1 Properties of aggregates.

Aggregate types	Specific weight (kg/m ³)	Water absorption (%)	Fineness modulus
Natural fine (NFA)	2.59	1.71	2.86
Recycled fine (RFA)	2.29	6.49	3.16
Natural coarse (NCA)	2.65	1.89	6.82

were within the requirements of the standard particle size distribution of ASTM C136 (2014).

The specific weight and water absorption of the aggregates were measured based on ASTM C127 (2015), and the fineness modulus was calculated according to ASTM C33 (2010). The measured properties are summarized in Table 1. In this study, the water absorption of RFA was 6.49%, which was three times higher than that of NFA. This was because of the old cement paste remaining on the surface of RFA. One notes that the water absorption of RFA used in this study was lower than that in the literatures, e.g. 8.5–13% (Evan-gelista and Brito 2007; Kumar et al. 2017; Kurda et al. 2017; Pereira et al. 2012b; Zega and Maio 2011). Such improvement may be resulted from RFA productions of a local manufacture (Sim and Won 2010; Won 2006; Won and Sim 2009). Thus, the quality of RFA can be considered to be improved owing to lower porosity than that in the previous studies.

Additionally, the limit of water absorption for recycled aggregates varies according to the design specification. For example, Korean Construction Specification (2016), Spanish Code (2008), and RILEM TC 121 (1994) recommend the maximum water absorption of 3–4%, 5%, and 10%, respectively. Canada Standard Association (CSA A23.1-09 2008) specifies that the maximum water absorption of recycled aggregates is 3% for high quality, 3–6% for medium grade, and 6% or higher for low grade. However, AASHTO MP 16 (2010), ACI 555-10 (2010), ASTM C33 (2010), and ASTM C33 (2016) do not provide a specific criterion for the water absorption of RFA. Thus, the measured water absorption was within the range specified in the RILEM TC 121 (1994), but it was higher than the ranges specified in Korean Construction Specification (2016), Spanish Code (2008), and CSA A23.1-09 (2008).

As binding materials of concrete, ordinary Portland cement (OPC), FA, and ground granulated blast-furnace slag (GGBS) were utilized. The chemical compositions of the binding materials were measured using X-ray fluorescence (XRF), and the specific surface area was evaluated according to ASTM C204 (2011), as presented in Table 2. These data were obtained from a manufacturer.

Table 2 Chemical compositions and physical properties of cement and pozzolanic admixtures.

	Ordinary Portland cement (OPC)	Fly ash (FA)	Ground granulated blast-furnace slag (GGBS)
Chemical composition (%)			
Al ₂ O ₃	5.77	15.14	21.22
CaO	61.43	39.48	11.49
Fe ₂ O ₃	3.36	0.91	6.57
K ₂ O	1.02	0	0.71
MgO	2.38	5.96	1.64
SiO ₂	21.62	34.25	52.09
SO ₃	2.10	3.51	1.44
Al ₂ O ₃	5.77	15.14	21.22
Specific surface area (m ² /kg)	362	352	408
Density	3.15	2.90	2.18

2.2 Mixing Proportions

The mixing proportions for NS and HS concrete were designed according to the change in the replacement ratio of RFA. The design strengths were 30 MPa and 60 MPa for NS and HS concrete, respectively. Five replacement ratios (i.e., 0%, 15%, 30%, 50%, and 100% by weight) were selected, resulting in a total of ten mixing proportions (see Table 3). Notably, concrete with zero replacement ratio of RFA, referred to as virgin concrete, provides the reference mechanical behaviors. The specimen IDs indicate the design strength and RFA replacement ratio. Aggregates were prepared under the SSD condition ASTM 128C (2015), and thus the effective w/c ratio was used in this study. Up to 10% and 20% of mineral admixtures of FA and GGBS, respectively, were added. These pozzolanic ingredients are known to reduce the hydration heats, which can decrease shrinkage cracks. Furthermore, they significantly improved the mechanical and durability properties of recycled aggregate concrete (Kumar et al. 2017). A high slump value was maintained for all the mixing proportions by calibrating the amount of polycarboxylate-based superplasticizer (SP). For NS concrete, 3.16–3.75 kg/m³ of SP was used, whereas 5.57–7.86 kg/m³ of SP was added to HS concrete.

The raw materials were mixed in three stages (Table 4). First, the fine and coarse aggregates were mixed in dry condition for 30 s. Subsequently, the binders were added and mixed for 30 s in dry condition. Finally, all the other materials were added and mixed for 90 s and 180 s for NS and HS concrete, respectively. Similar mixing processes were employed to guarantee denser concrete and improve the ITZ characteristics of the recycled

Table 3 Mixture proportions of NS and HS concrete.

Specimen ID	S/a (%)	W/B (%)	Unit weight (kg/m ³)								
			W	OPC	FA	GGBS	NS	RS	G	SP	AE ^a
NS concrete											
30-R0	48.0	42.5	168	277	40	79	832	0	922	3.75	0.6
30-R15							707	110		3.75	
30-R30							582	221		3.16	
30-R50							416	368		3.16	
30-R100							0	736		3.16	
HS concrete											
60-R0	43.0	25.0	164	459	66	131	652	0	885	7.86	0.79
60-R15							555	87		7.86	
60-R30							457	173		7.53	
60-R50							326	288		7.53	
60-R100							0	577		5.57	

^a Water reducing agent.

Table 4 Mixing procedures and time for RFA concrete.

	Stage I Aggregates (s)	Stage II Aggregates + binder (s)	Stage III Aggregates + binder + water + chemical admixtures (s)
NS concrete	30	30	90
HS concrete	30	30	180

aggregates (Brand et al. 2015; Kou and Poon 2008). Subsequently, the slump and air content were measured, as summarized in Table 5. For NS concrete, the average slump and air content were 214 ± 5.5 mm and 5.3 ± 0.2%, respectively. The HS concrete demonstrated the average slump of 217 ± 2.4 mm and the air content of 3.4 ± 0.2%.

2.3 Specimen Fabrication and Curing

To measure the compressive strength, splitting strength, and elastic modulus, 180 cylinder specimens were fabricated. The diameter and length of the cylinders were 100 mm and 200 mm, respectively. A day after the specimen fabrication, the specimens were demolded and exposed to air-dry conditions. For the shrinkage strain measurement, twenty prism specimens (100 × 100 × 400 mm) were fabricated. Strain gauges were embedded at the center of the prism specimens along the longitudinal direction. After the prism specimens were demolded, they were placed in a temperature and humidity chamber at a constant temperature of 23.8 ± 0.4 °C and relative humidity of 52.5 ± 1.0% for 260 days.

Table 5 Air content and slump measurement results.

Specimen ID	Air content (%)		Slump (mm)	
	Measured	Avg. (COV)	Measured	Avg. (COV)
NS concrete				
30-R0	5.2	5.3 ± 0.21 (4.0%)	210	214 ± 5.5 (2.6%)
30-R15	5.6		220	
30-R30	5.0		220	
30-R50	5.3		215	
30-R100	5.5		205	
HS concrete				
60-R0	3.7	3.3 ± 0.24 (7.2%)	220	217 ± 2.4 (1.1%)
60-R15	3.3		215	
60-R30	3.0		215	
60-R50	3.5		220	
60-R100	3.2		215	

2.4 Tests for Compressive Strength, Splitting Tensile Strength, and Modulus of Elasticity

The compressive strength tests were conducted according to ASTM C39 (2015) at 3, 7, 28, and 190 days. A load was applied with the loading rate of 0.3 MPa/s using a universal testing machine (UTM). The splitting tensile strength was tested at 28 and 190 days based on ASTM C496 (2005). Two pieces of plywood of size (3 × 25 × 210 mm) were placed on each side of the cylinder. A load was applied with the loading rate of 1.4 MPa/min using the UTM. The modulus of elasticity was measured at 190 days in compliance with ASTM C469 (2014).

2.5 Drying Shrinkage Strain Measurement

Using the embedded strain gauge with a data acquisition system, the strains in the prism specimens were automatically recorded up to a period of 260 days. Twenty specimens were tested, and for each mixing proportion, the average strain of the two replicate specimens was used as the representative shrinkage strain.

3 Test Results

3.1 Compressive Strength

The measured compressive strengths for NS and HS concrete are summarized in Table 6. The ratio of the compressive strength of RFA concrete to that of virgin concrete is shown in Fig. 2 (Note: the result of 60-R100 was not included because of a data acquisition problem). The test results revealed that, as expected, the compressive strength increased with the increase in curing time. The strength of RFA concrete generally decreased as the replacement ratio of RFA increased. In addition, the strength decrement ratios at the various curing stages were similar for each replacement ratio, as shown in Fig. 2. For NS concrete, the compressive strength of RFA concrete ($f'_{c(RFA)}$) decreased approximately 30% compared with that of virgin concrete ($f'_{c(NFA)}$) when NFA was completely replaced by RFA. For HS concrete, the maximum strength reduction ratio was approximately 10%, when the replacement ratio increased to 100%. Thus, it was observed that the increase of the RFA replacement ratio did not significantly reduce the compressive strength of HS concrete.

3.2 Splitting Tensile Strength

The results of the splitting tensile test are shown in Table 7. NS concrete exhibited a reduction in the splitting tensile strength with the increase in the replacement ratio of RFA, but no significant change was evident for

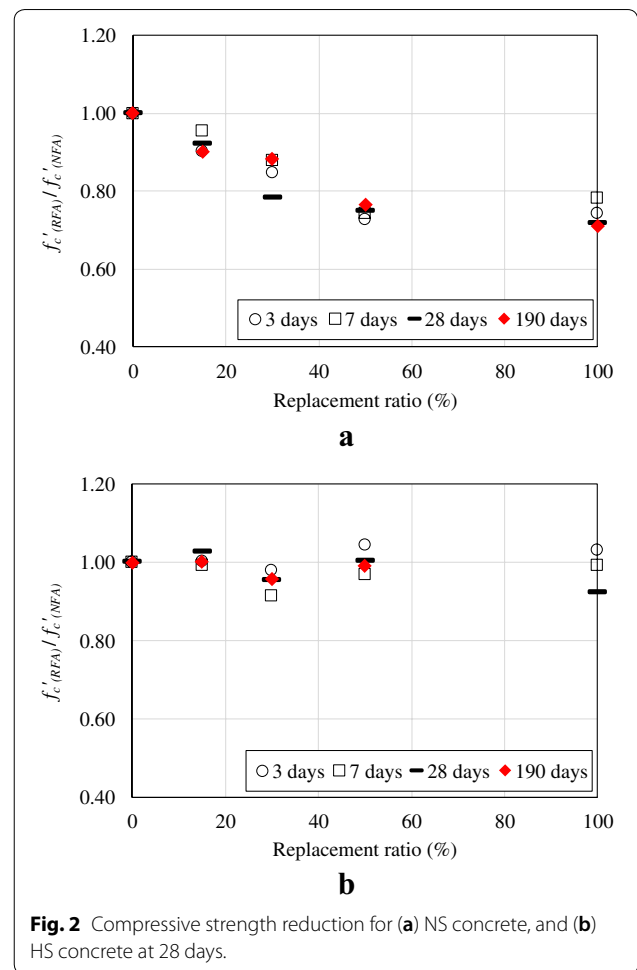


Fig. 2 Compressive strength reduction for (a) NS concrete, and (b) HS concrete at 28 days.

HS concrete. These behaviors are similar to the compressive strength results. It was observed that for HS concrete, the amount of RFA did not affect the tensile strength significantly, particularly when the curing time was sufficient, i.e., 190 days or longer.

Table 6 Compressive strength results (Unit: MPa).

Specimen ID	3 days		7 days		28 days		190 days	
	Measured	Avg. (COV)						
30-R0	18.6/17.6/19.2	18.5 ± 0.7 (3.8%)	25.5/25.9/25.8	25.7 ± 0.2 (0.8%)	45.4/47.5/47.7	46.9 ± 1.0 (2.1%)	49.0/59.8/57.1	55.3 ± 4.6 (8.3%)
30-R15	16.4/16.8/16.8	16.7 ± 0.2 (1.2%)	24.0/24.8/24.9	24.6 ± 0.4 (1.6%)	45.0/41.7/42.6	43.1 ± 1.4 (3.2%)	49.4/50.2/-	49.8 ± 0.4 (0.8%)
30-R30	15.5/15.6/15.8	15.6 ± 0.1 (0.6%)	23.7/21.6/22.5	22.6 ± 0.9 (4.0%)	37.4/33.3/39.4	36.7 ± 2.5 (6.8%)	48.8/45.5/52.3	48.9 ± 2.8 (5.7%)
30-R50	13.1/13.4/13.8	13.4 ± 0.3 (2.2%)	18.5/20.0/18.8	19.1 ± 0.6 (3.1%)	35.5/35.8/34.0	35.1 ± 0.8 (2.3%)	43.4/43.2/40.3	42.3 ± 1.4 (3.3%)
30-R100	13.8/13.9/13.4	13.7 ± 0.2 (1.5%)	20.0/20.4/20.0	20.1 ± 0.2 (1.0%)	33.8/33.2/33.6	33.5 ± 0.2 (0.6%)	41.5/37.1/-	39.3 ± 2.2 (5.6%)
60-R0	42.6/40.5/40.6	41.2 ± 1.0 (2.4%)	51.0/51.5/50.2	50.9 ± 0.5 (1.0%)	69.1/64.9/66.7	66.9 ± 1.7 (2.5%)	80.2/81.2/77.5	79.6 ± 1.6 (2.0%)
60-R15	40.5/41.8/41.8	41.4 ± 0.6 (1.5%)	52.4/48.4/50.8	50.5 ± 1.6 (3.2%)	69.8/70.5/65.4	68.6 ± 2.3 (3.4%)	80.5/79.2/79.4	79.7 ± 0.6 (7.5%)
60-R30	40.1/39.9/41.2	40.4 ± 0.6 (1.5%)	46.2/46.4/47.0	46.5 ± 0.3 (6.5%)	61.0/65.4/65.1	63.8 ± 2.0 (3.1%)	76.4/76.4/75.7	76.2 ± 0.3 (0.4%)
60-R50	43.2/42.7/43.4	43.1 ± 0.3 (0.7%)	49.5/48.2/50.2	49.3 ± 0.8 (1.6%)	67.4/66.3/67.7	67.1 ± 0.6 (0.9%)	80/76.9/80	79.0 ± 1.5 (1.9%)
60-R100	42.1/43.3/42.2	42.5 ± 0.5 (1.2%)	51.5/50.6/49.3	50.5 ± 0.9 (1.8%)	65.8/55.2/64.0	61.7 ± 4.6 (7.5%)	-/-/-	-

Table 7 Measured splitting tensile strength and elastic modulus.

Specimen ID	Splitting tensile strength (MPa)				Elastic modulus (MPa)	
	28 days		190 days		190 days	
	Measured	Avg. (COV)	Measured	Avg. (COV)	Measured	Avg. (COV)
30-R0	3.8/4.1/–	3.9 ± 0.1 (2.6%)	4.8/5.4/3.4	4.5 ± 0.8 (17.8%)	32.5/30.1/35.9	32.5 ± 2.4 (7.4%)
30-R15	3.2/3.1/–	3.2 ± 0.0 (0.0%)	5.1/4.4/–	4.8 ± 0.4 (8.3%)	28.3/–/–	28.3
30-R30	3.3/3.6/4.1	3.7 ± 0.3 (8.1%)	4.0/4.7/4.1	4.3 ± 0.3 (7.0%)	33.2/32.5/31.6	32.4 ± 0.7 (2.2%)
30-R50	3.5/3.6/3.4	3.5 ± 0.1 (2.9%)	4.5/4.5/4.3	4.4 ± 0.1 (2.3%)	32.9/25.2/17.2	25.1 ± 6.4 (25.5%)
30-R100	3.8/3.4/3.1	3.4 ± 0.3 (8.8%)	4.4/3.7/4.3	4.1 ± 0.3 (7.3%)	20.5/–/–	20.5
60-R0	4.6/5.1/–	4.9 ± 0.3 (6.1%)	6.2/4.6/5.3	5.4 ± 0.7 (13.0%)	35.7/37.1/32.8	35.2 ± 1.8 (5.1%)
60-R15	4.8/5.3/6.2	5.4 ± 0.6 (11.1%)	5.7/5.0/5.5	5.4 ± 0.3 (5.6%)	–/–/–	N/A
60-R30	5.3/5.7/–	5.5 ± 0.2 (3.6%)	5.4/5.3/5.5	5.4 ± 0.1 (1.9%)	40.5/33.5/28.9	34.3 ± 4.8 (14.0%)
60-R50	4.4/4.6/–	4.5 ± 0.1 (2.2%)	5.7/5.5/5.2	5.5 ± 0.2 (3.6%)	34.2/32.3/36.6	34.4 to ± 1.7 (4.9%)
60-R100	4.8/4.7/4.7	4.7 ± 0.1 (2.1%)	5.5/5.4/–	5.5 ± 0.1 (1.8%)	–/–/–	N/A

3.3 Modulus of Elasticity

To measure the modulus of elasticity, the compressive stress versus strain relationship was measured (Fig. 3). The elastic modulus was then calculated using a chord modulus ASTM C469 (2014), which is the slope of two specified points on a stress–strain curve. One point is specified to be where the compressive stress is 40% of the compressive strength, and the other point is at the compressive strain of 5.0×10^{-5} . The calculated modulus of elasticity is summarized in Table 7. The results showed that for NS concrete, the elastic modulus generally decreased with an increase in the RFA replacement ratio. However, the variation in the elastic modulus of HS concrete was insignificant for the different replacement ratios.

3.4 Drying Shrinkage Strain

Figure 4 shows the measured shrinkage strains for NS and HS concrete. The drying shrinkage strain of RFA concrete exhibited a smaller increase after 28 days. The maximum shrinkage strain for the samples with 100% RFA replacement ratio was measured to be below 1000 $\mu\epsilon$ for NS concrete and 800 $\mu\epsilon$ for HS concrete. These results are similar to those for virgin concrete (i.e., 200–800 $\mu\epsilon$) as reported by ACI 209-05 (2005). The maximum shrinkage strain difference between virgin concrete and RFA concrete was approximately 200 $\mu\epsilon$ at 260 days, which is equivalent to 5.7% of the ultimate compressive strain of concrete (i.e., 3500 $\mu\epsilon$).

For RFA concrete, the drying shrinkage strain increased along with increase in its replacement ratio and was more than that of virgin concrete. This may be because a higher RFA replacement ratio results in a higher water content in concrete owing to RFA’s higher water absorption.

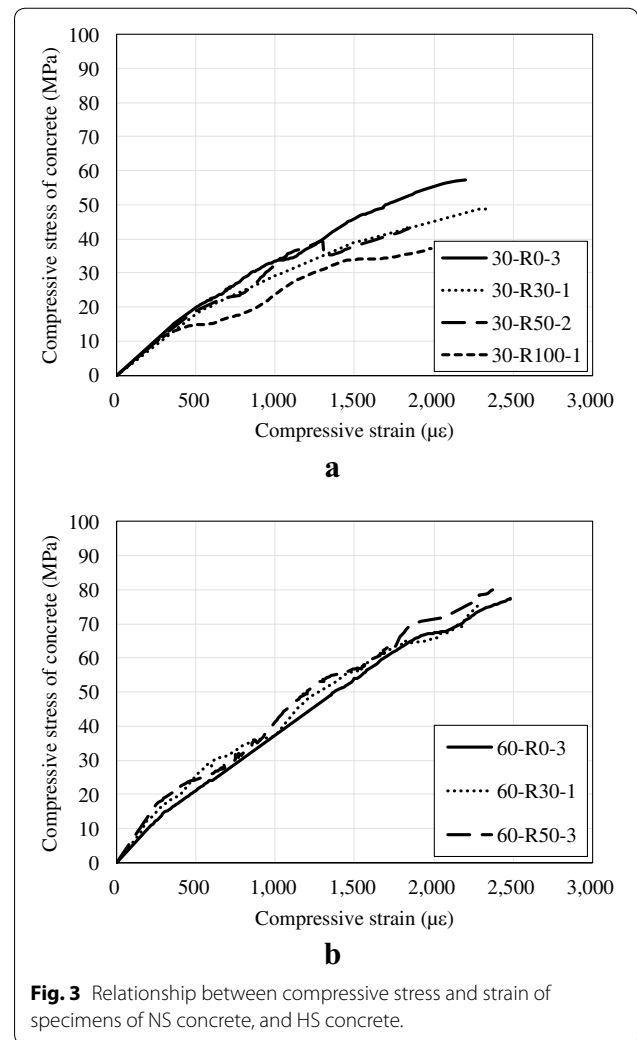
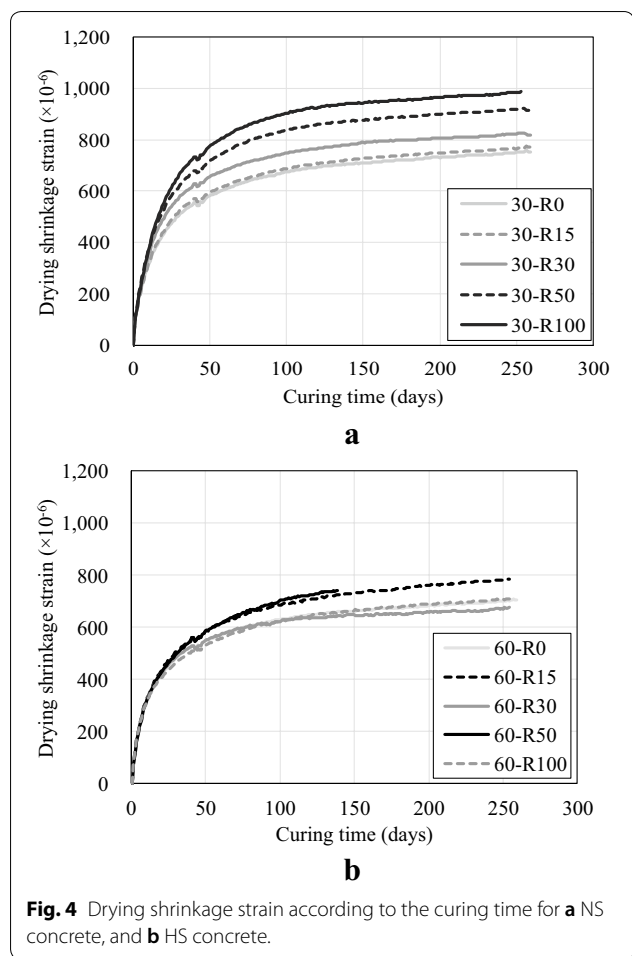


Fig. 3 Relationship between compressive stress and strain of specimens of NS concrete, and HS concrete.

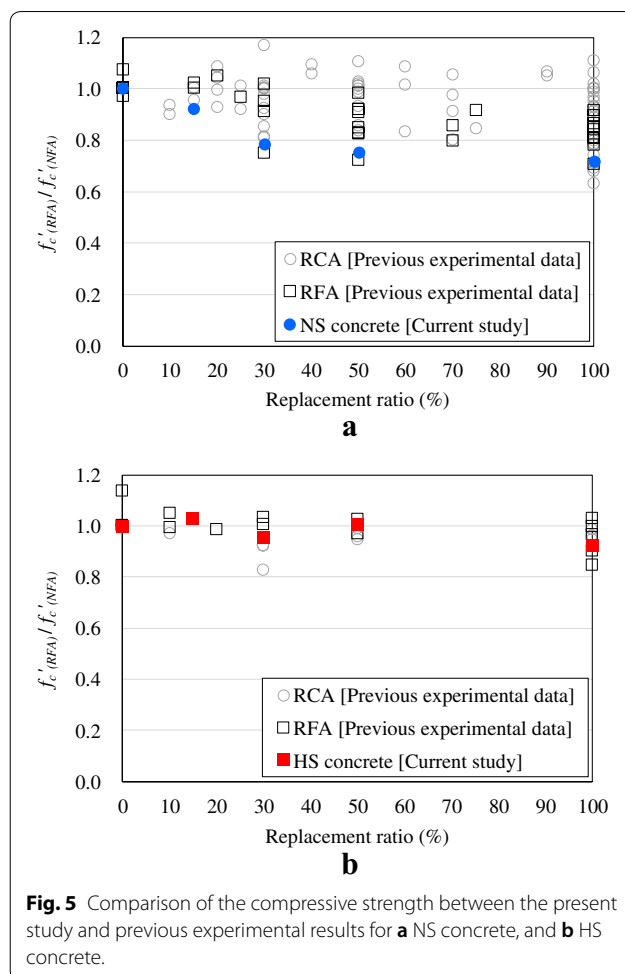


HS concrete had a smaller drying shrinkage strain than NS concrete. This is because a larger amount of binding materials with similar water content (see Table 3) provides a denser microstructure, and thus, the effect of the replacement ratio on shrinkage strain was not significant for HS concrete.

4 Discussion

4.1 Effects of RFA Replacement Ratio on Concrete Compressive Strength

The average compressive strength variations for NS and HS concrete according to the replacement ratio of RFA are plotted in Fig. 5. Additionally, the previous experimental data for RFA concrete (Evangelista and Brito 2007; Kumar et al. 2017; Kurda et al. 2017; Pedro et al. 2017; Pereira et al. 2012a, b; Santos et al. 2017; Tahar et al. 2017; Yang et al. 2008; Zega and Maio 2011) and RCA concrete (Arezoumandi et al. 2015; Chen et al. 2016; Etxeberria et al. 2007; Folino and Xargay 2014; Kanellopoulos et al. 2014; Knaack and Kurama 2014; Kurda et al. 2017; Montero and Laserna 2017; Pedro et al. 2017; Tahar



et al. 2017; Tam et al. 2015; Xie and Ozbakkaloglu 2016) are included for comparison. Both the current and previous experimental data for RFA concrete showed that compressive strength decreases with an increase in the RFA replacement ratio. However, the previous experimental data for RCA concrete showed that the decreased in compressive strength was insignificant, and the strength deviation tended to increase with an increase in the RCA replacement ratio for NS concrete.

In addition, for RFA concrete, the decrease in strength for HS concrete was smaller than that of NS concrete (see Fig. 5). Thus, the RFA replacement ratio may not affect the compressive strength of HS concrete significantly. The different decreases in strength for NS and HS concrete may be associated with the different failure mechanisms.

Regarding the compressive failure of NS concrete, microcracks are generally formed along the interface between the paste and aggregate, i.e., ITZ. Thus, the failure surface generally corresponds to the boundary between the cement paste and aggregate. Thus, the

bonding strength along ITZ may affect the compressive strength of NS concrete. The ITZ characteristics of RFA concrete may not be as good as those of virgin concrete because of the old cement paste remaining on the RFA surface. Therefore, the compressive strength of NS concrete decreased with the increase in the RFA replacement ratio.

For HS concrete, the failure surface does not always correspond to the boundary between the cement paste and aggregate. In other words, the interfacial strength along ITZ may be sufficiently high because of the dense hydrated components caused by a higher amount of binding materials, and thus the concrete material failure can be observed through grains of aggregates rather than ITZ. Basically, the compressive failure may be governed by other defects in concrete. Although ITZ characteristics of RFA concrete may not be as good as those of virgin concrete, the decrease in the compressive strength owing to RFA replacement was insignificant in this study, particularly for HS concrete.

Figure 6 shows the development of compressive strength for NS and HS concrete according to the curing time. As the curing time increased, the compressive strength increased, as expected. The compressive strength of the test specimens increased by approximately 15–30% for NS concrete and 15–20% for HS concrete at 190 days compared with the strength at 28 days. The strength ratios for a specified day (t_{day}), i.e., $f'_c(t_{day})/f'_c(28)$, were similar for NS and HS concrete in this study regardless of the RFA replacement ratio. Similarly, the development of the splitting tensile strength for NS and HS concrete at 190 days is illustrated in Fig. 7. The ratio of the splitting strength at 190 days to that at 28 days for NS concrete was higher than that for HS concrete. This was similar to the variation in the compressive strength ratios for NS and HS concrete. The ratio of the tensile strength at 28 days to that at 190 days was approximately 1.25 for NS concrete and 1.15 for HS concrete.

4.2 Relation Between Splitting Tensile Strength and Compressive Strength

The ratio of the tensile strength to the compressive strength according to the RFA replacement ratio is summarized in Table 8. The strength ratios were on an average 8–10% for NS concrete and 6–7% for HS concrete. These were within the general range of the splitting strength ratio of concrete (Mindess and Young 2003). In addition, the tensile strength ratio with respect to that of virgin concrete slightly increased along with the increase in the replacement ratio of RFA. This is because the reduction in the tensile strength of RFA concrete is less sensitive than the reduction in the compressive strength of NS concrete. However, there was no significant change

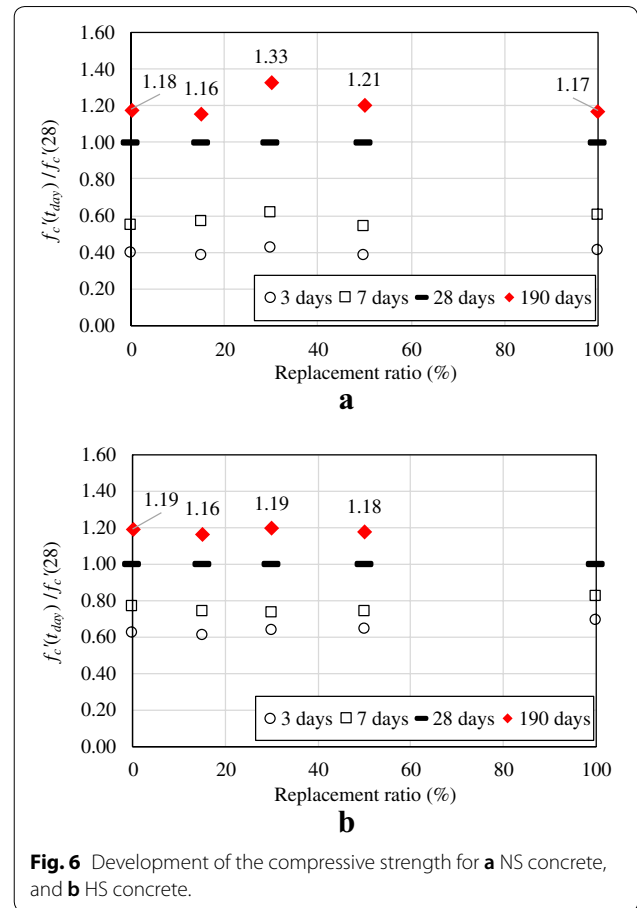


Fig. 6 Development of the compressive strength for **a** NS concrete, and **b** HS concrete.

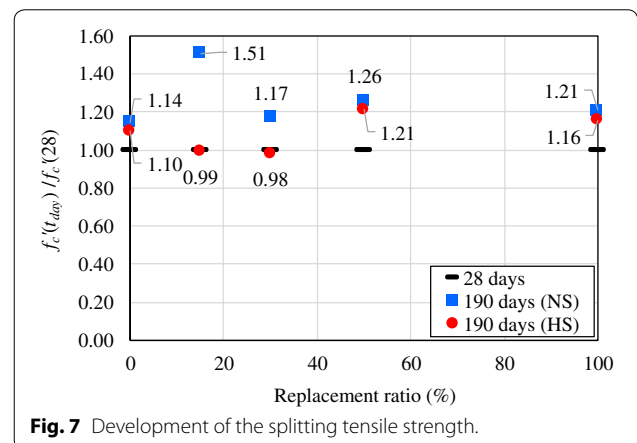


Fig. 7 Development of the splitting tensile strength.

for HS concrete. This is because the compressive and tensile strengths did not vary significantly with the increase in the RFA replacement ratio.

The splitting tensile strength may be approximated using the compressive strength of RFA concrete with empirical equations, summarized in Table 9 (ACI 318-14 (2014); ACI 363-10 (2010); Carino and Lew 1982;

Table 8 Relationship between the tensile strength and the compressive strength according to the curing time.

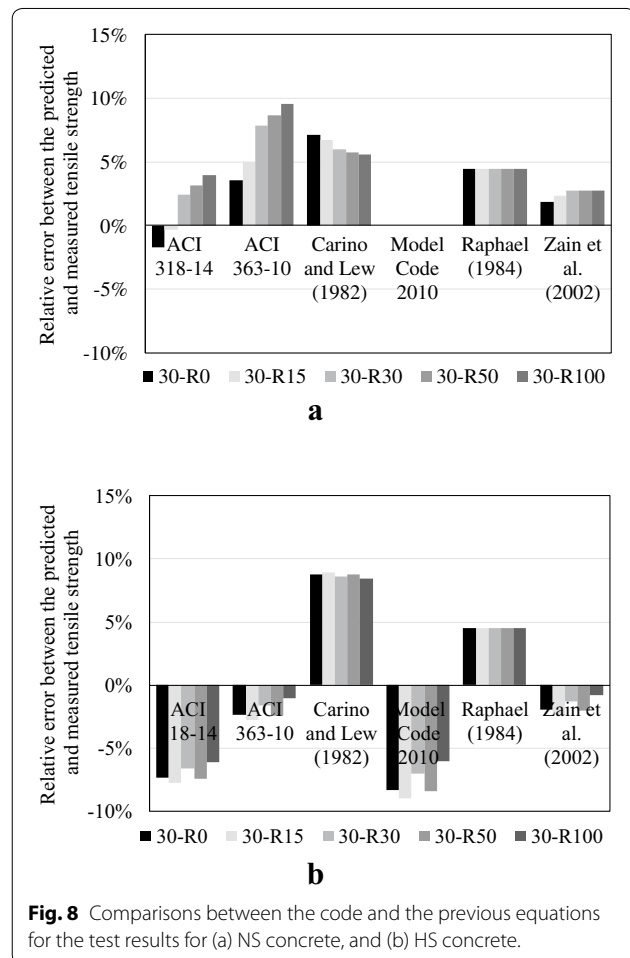
Specimens ID	28 days			190 days		
	Avg. f'_c (MPa)	Avg. f_{st} (MPa)	f_{st}/f'_c (%)	Avg. f'_c (MPa)	Avg. f_{st} (MPa)	f_{st}/f'_c (%)
30-R0	46.9	3.9	8.3	55.3	4.5	8.1
30-R15	43.1	3.2	7.4	49.8	4.8	9.6
30-R30	36.7	3.7	10.1	48.9	4.3	8.8
30-R50	35.1	3.5	10.0	42.3	4.4	10.4
30-R100	33.5	3.4	10.1	39.3	4.1	10.4
60-R0	66.9	4.9	7.3	79.6	5.4	6.8
60-R15	68.6	5.4	7.9	79.7	5.4	6.8
60-R30	63.8	5.5	8.6	76.2	5.4	7.1
60-R50	67.1	4.5	6.7	79.0	5.5	7.0
60-R100	61.7	4.7	7.6	–	–	–

Table 9 Prediction equation of the splitting tensile strength.

References	Equations
ACI 318-14 (2014)	$0.56\sqrt{f'_c}$
ACI 363-10 (2010)	$0.59\sqrt{f'_c}$
Carino and Lew (1982)	$0.272(f'_c)^{0.71}$
Model Code (2010)	$2.12\ln(1 + 0.1(f'_c + 8))$
Raphael (1984)	$0.313(f'_c)^{0.667}$
Zain et al. (2002)	$f'_c / (0.1f'_c + 7.11)$

Raphael 1984; Zain et al. 2002). It is noteworthy that these equations were initially developed for virgin concrete. The differences between the measured splitting tensile strength and approximated strength are plotted in Fig. 8. In general, the empirical equations from the design standards (ACI 318-14 2014; Model Code 2010) marginally underestimated the splitting tensile strength for HS concrete. The differences between the measured strength and approximated strength were less than 10% in most cases. Furthermore, based on the previous and current experimental data, the relationship between the measured splitting tensile strength and the compressive strength is plotted in Fig. 9. Although the tensile strength of the current study was slightly higher than that of the previous work, the measured tensile strength displayed similar trends according to the measured compressive strength. Then, a regression analysis provides the following empirical expression

$$f_{st} = 0.557\sqrt{f'_c} \tag{1}$$



for the approximation of the splitting tensile strength for a given compressive strength. One notes that the obtained expression is similar to the equation from ACI 318-14 (2014), as shown in Fig. 9. Accordingly, the

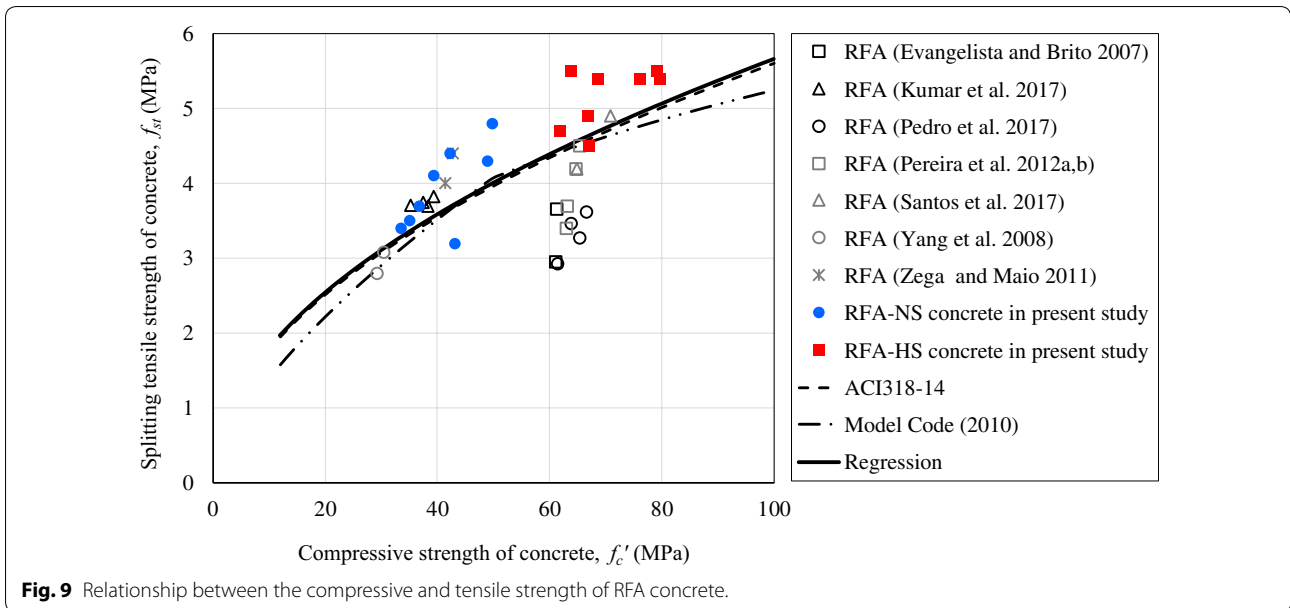


Fig. 9 Relationship between the compressive and tensile strength of RFA concrete.

existing empirical equations of virgin concrete can be utilized to estimate the splitting tensile strength of RFA concrete.

4.3 Relation Between Elastic Modulus and Compressive Strength

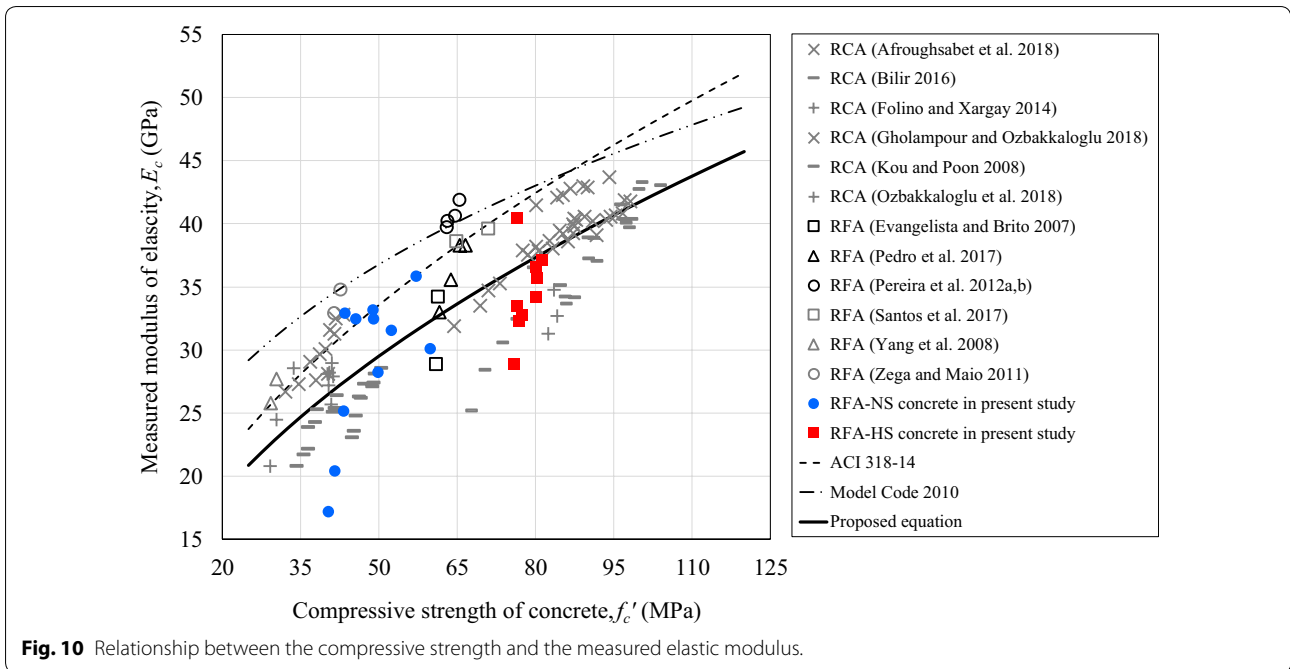
The modulus of elasticity can be estimated from the compressive strength of RFA concrete by using an empirical equation, as illustrated in Table 10. Two empirical equations provided by ACI 318-14 (2014) and Model Code (2010) for virgin concrete were employed in this study. The comparison illustrated that the ACI 318-14 (2014) and Model Code (2010) equations overestimated the elastic modulus of NS concrete containing RFA.

The relationships between the measured compressive strength and measured modulus of elasticity are presented in Fig. 10. The present experimental results for RFA concrete are denoted by solid markers. The previous experimental data for RCA concrete (Afroughsabet et al. 2018; Bilir 2016; Folino and Xargay 2014; Gholam-pour and Ozbakkaloglu 2018; Kou and Poon 2013; Ozbakkaloglu et al. 2017) and RFA concrete (Evangelista and Brito 2007; Pedro et al. 2017; Pereira et al. 2012a, b; Santos et al. 2017; Yang et al. 2008; Zega and Maio 2011) are indicated with empty markers for comparison. The comparison demonstrated that the ratios of the elastic modulus to the compressive strength for RFA concrete were like those for RCA concrete. From the comparative study,

Table 10 Estimated elastic modulus using the code equations.

Specimen ID	ACI 318-14 (2014) ^a		Model Code (2010) ^b	
	$E_c = 4.7\sqrt{f'_c}$		$E_c = 21.5(f'_c/10)^{1/3}$	
	Calculated (GPa)	Avg. (GPa)	Calculated (GPa)	Avg. (GPa)
30-R0	32.9/36.3/35.5	34.9	36.5/39.0/38.4	38.0
30-R15	33.0/33.3/-	33.2	36.7/36.8/-	36.7
30-R30	32.8/31.7/34.0	32.8	36.5/35.6/37.3	36.5
30-R50	31.0/30.9/29.8	30.6	35.1/35.0/34.2	34.8
30-R100	30.3/28.6/-	29.5	34.6/33.3/-	33.9
60-R0	42.1/42.4/41.4	41.9	43.0/43.2/42.5	42.9
60-R15	42.2/41.8/41.9	42.0	43.1/42.9/42.9	42.9
60-R30	41.1/41.1/40.9	41.0	42.3/42.3/42.2	42.3
60-R50	42.0/41.2/42.0	41.8	43.0/42.4/43.0	42.8

^a $f'_c \geq 17$ MPa, ^b $f'_c \geq 12$ MPa.



it is concluded that the RFA concrete used in this study can have effective structural stiffness as a structural concrete member. This is similar to RCA concrete, which has been utilized as a structural concrete member.

Furthermore, in this study, an empirical equation is proposed to estimate the elastic modulus of RFA (or RCA) concrete. This is because the design equations overestimated the measured elastic modulus, particularly for NS concrete (Fig. 10). The following expression for the elastic modulus of concrete with recycled concrete aggregates is obtained based on regression analysis:

$$E_c = 4.175\sqrt{f'_c} \quad (2)$$

which is indicated as a solid line in Fig. 10.

5 Conclusions

This study investigated the mechanical behaviors of NS and HS concrete containing RFA. In the experiment, the five replacement ratios of RFA with a high slump property were employed. The compressive strength, tensile strength, elastic modulus, and drying shrinkage strain of RFA concrete were measured. Based on the experimental results, the key findings are summarized as follows:

- The compressive strength of RFA concrete decreased by approximately 30% and 10% for NS and HS concrete, respectively, as the replacement ratio of RFA increased from 0 to 100%. Similarly, the elastic mod-

ulus of NS concrete decreased with the increase in the RFA replacement ratio. However, the variation in the elastic modulus of HS concrete was not significant. The decreases in the compressive strength and elastic modulus for NS concrete were larger than those for HS concrete. These differences between NS and HS concrete may be resulted from the different failure mechanisms associated with ITZ.

- The ratios of the elastic modulus to the compressive strength for RFA concrete were similar to those for RCA concrete. However, the design equations of ACI 318-14 (2014) and Model Code (2010) overestimated the elastic modulus of RFA (and RCA) concrete for a specified compressive strength. Therefore, an empirical expression was suggested to approximate the elastic modulus of RFA concrete.
- The rate of compressive strength development was consistent regardless of the RFA replacement ratio. The average ratio of the compressive strength at 190 days to that at 28 days was 1.15–1.3, and the ratio of tensile strength at 190 days to that at 28 days was 1.15–1.25, demonstrating good strength development. Good compressive and tensile strength developments were demonstrated for long-term curing.
- Regardless of the curing time and replacement ratio of RFA, the ratio of the splitting tensile strength to the compressive strength of RFA concrete was similar to the corresponding ratio for ordinary concrete. Thus, the existing empirical equations for ordinary concrete, e.g., ACI 318-14 (2014) and Model Code

(2010) can be used to approximate the indirect tensile strength of RFA concrete.

- The measured drying shrinkage strain of RFA concrete with 100% replacement ratio was within the strain range reported by ACI 209-05 (2005). The increase in RFA content resulted in the increase in the drying shrinkage strain. However, the increase in shrinkage owing to the use of RFA was at most 250 $\mu\epsilon$, which is 5–6% of the ultimate compressive strain of concrete. Thus, the shrinkage strain may not have a harmful effect on NS and HS concrete with RFA so that it may not be a significant issue for the potential use of RFA concrete as a concrete member, e.g., as filled structural concrete.

Authors' contributions

MJ planned the experimental program, performed experiments, analyzed data, and drafted the paper. KP analyzed experimental data and organized and drafted the paper. WJP planned the experimental program for RFA concrete. All authors read and approved the final manuscript.

Funding

This research was supported by Basic Science Research Program through the National Research Foundation of Korea (NRF) funded by the Ministry of Science, ICT & Future Planning (NRF-2016R1D1A1B03934809), and by the Korea Institute of Energy Technology Evaluation and Planning (KETEP) funded by the Ministry of Trade, Industry & Energy (#20171510101910). The information presented in this paper is the opinion of solely the authors and does not necessarily reflect the views of the sponsoring agency.

Availability of data and materials

The experimental data used to support the observations of this study are included in the article.

Competing interests

The authors declare that they have no competing interests.

Author details

¹ Department of Civil and Environmental Engineering, Yonsei University, Seoul, Republic of Korea. ² Department of Architectural Engineering, Kangwon National University, Samcheok, Republic of Korea.

Received: 31 March 2019 Accepted: 21 September 2019

Published online: 02 December 2019

References

- AASHTO MP 16. (2010). *Standard specification for reclaimed concrete aggregate for use as coarse aggregate in hydraulic cement concrete*. Washington D.C.: American Association of State Highway and Transportation Officials.
- ACI Committee 209. (2005). *Report on factors affecting shrinkage and creep of hardened concrete (ACI 209-05)*. Farmington Hills: American Concrete Institute.
- ACI Committee 318. (2014). *Building code requirements for structural concrete and commentary (ACI 318-14)*. Farmington Hills: American Concrete Institute.
- ACI Committee 363. (2010). *State of the art report on high-strength concrete (ACI 363R-10)*. Farmington Hills: American Concrete Institute.
- ACI Committee 555. (2010). *Removal and reuse of hardened concrete (ACI 555-10)*. Farmington Hills: American Concrete Institute.
- Afroughsabet, V., Biolzi, L., & Monteiro, P. J. M. (2018). The effect of steel and polypropylene fibers on the chloride diffusivity and drying shrinkage of high-strength concrete. *Composites Part B: Engineering*, 139, 84–96.
- Alves, A. V., Vieira, T. F., Brito, J., & Correia, J. R. (2014). Mechanical properties of structural concrete with fine recycled ceramic aggregates. *Construction and Building Materials*, 64, 103–113.
- Arezoumandi, M., Smith, A., Volz, J. S., & Khayat, K. H. (2015). An experimental study on flexural strength of reinforced concrete beams with 100% recycled concrete aggregate. *Engineering Structures*, 88, 154–162.
- ASTM C127. (2015). *Standard test method for relative density (specific gravity) and absorption of coarse aggregate—ASTM subcommittee C09.20*. West Conshohocken: ASTM International.
- ASTM C128. Society for Testing and Materials. ASTM C128. (2015). *American Standard test method for relative density (specific gravity) and absorption of fine aggregate*. West Conshohocken: ASTM International.
- ASTM C136. American Society for Testing and Materials. ASTM C136/C136M. (2014). *Standard Test method for Sieve analysis of fine and coarse aggregates*. West Conshohocken: ASTM International.
- ASTM C204. (2011). *Standard test methods for fineness of hydraulic cement by air-permeability*. West Conshohocken: ASTM International.
- ASTM C33. (2010). *Standard specification for concrete aggregates*. West Conshohocken: ASTM International.
- ASTM C39. (2015). *Compressive strength of cylindrical concrete specimens*. West Conshohocken: ASTM International.
- ASTM C469. (2014). Standard test method for static modulus of elasticity and Poisson's ratio of concrete in compression. *ASTM International*. <https://www.astm.org>
- ASTM C496. (2005). E662 standard test method for specific optical density of smoke generated by solid materials. *Annual Book of ASTM Standards*
- Bilir, T. (2016). Investigation of performances of some empirical and composite models for predicting the modulus of elasticity of high strength concretes incorporating ground pumice and silica fume. *Construction and Building Materials*, 127, 850–860.
- Brand, A. S., Roesler, J. R., & Salas, A. (2015). Initial moisture and mixing effects on higher quality recycled coarse aggregate concrete. *Construction and Building Materials*, 79, 83–89.
- Carino, N. J., & Lew, H. S. (1982). Re-examination of the relation between splitting tensile and compressive strength of normal weight concrete. *ACI Materials Journal*, 79(3), 214–219.
- Chen, G. M., He, Y. H., Jiang, T., & Lin, C. J. (2016). Behavior of CFRP-confined recycled aggregate concrete under axial compression. *Construction and Building Materials*, 111, 85–97.
- Choi, H., Choi, H., Lim, M., Inoue, M., Kitagaki, R., & Noguchi, T. (2016). Evaluation on the mechanical performance of low-quality recycled aggregate through interface enhancement between cement matrix and coarse aggregate by surface modification technology. *International Journal of Concrete Structures and Materials*, 10(1), 87–97.
- CSA A23.1-09. (2008). *Concrete materials and methods of concrete construction*. Ottawa: Canadian Standards Association.
- Etzeberria, M., Vázquez, E., Mari, A., & Barra, M. (2007). Influence of amount of recycled coarse aggregates and production process on properties of recycled aggregate concrete. *Cement and Concrete Research*, 37(5), 735–742.
- Evangelista, L., & Brito, J. (2007). Mechanical behaviour of concrete made with fine recycled concrete aggregates. *Cement & Concrete Composites*, 29(5), 397–401.
- Folino, P., & Xargay, H. (2014). Recycled aggregate concrete—Mechanical behavior under uniaxial and triaxial compression. *Construction and Building Materials*, 56, 21–31.
- Gholampour, A., & Ozbakkaloglu, T. (2018). Time-dependent and long-term mechanical properties of concretes incorporating different grades of coarse recycled concrete aggregates. *Engineering Structures*, 157, 224–234.
- Gómez-Soberón, J. M. V. (2002). Porosity of recycled concrete with substitution of recycled concrete aggregate: An experimental study. *Cement and Concrete Research*, 32(8), 1301–1311.
- Kanellopoulos, A., Nicolaidis, D., & Petrou, M. F. (2014). Mechanical and durability properties of concretes containing recycled lime powder and recycled aggregates. *Construction and Building Materials*, 53, 253–259.
- Katz, A. (2003). Properties of concrete made with recycled aggregate from partially hydrated old concrete. *Cement and Concrete Research*, 33(5), 703–711.

- Knaack, A. M., & Kurama, Y. C. (2014). Behavior of reinforced concrete beams with recycled concrete coarse aggregates. *Journal of Structural Engineering*, 141(3), B4014009.
- Korean Construction Specification. (2016). *Recycled aggregate concrete*. Infrastructure and Transport of Korea: Ministry of Land.
- Kou, S. C., & Poon, C. S. (2008). Mechanical properties of 5-year-old concrete prepared with recycled aggregates obtained from three different sources. *Magazine of Concrete Research*, 60(1), 57–64.
- Kou, S. C., & Poon, C. S. (2013). Long-term mechanical and durability properties of recycled aggregate concrete prepared with the incorporation of fly ash. *Cement & Concrete Composites*, 37(1), 12–19.
- Kumar, R., Gurram, S. C. B., & Minocha, A. K. (2017). Influence of recycled fine aggregate on microstructure and hardened properties of concrete. *Magazine of Concrete Research*, 69(24), 1288–1295.
- Kurda, R., Brito, J., & Silvestre, J. D. (2017). Indirect evaluation of the compressive strength of recycled aggregate concrete with high fly ash ratios. *Magazine of Concrete Research*, 70(4), 204–216.
- McNeil, K., & Kang, T. H. K. (2013). Recycled concrete aggregates: A review. *International Journal of Concrete Structures and Materials*, 7(1), 61–69.
- Mindess, S., Young, J. F., & Darwin, D. (2003). *Concrete* (2nd ed.). Upper saddle River: Prentice Hall.
- Model Code. (2010). *Fib model code for concrete structures*. Berlin: Ernst & Sohn.
- Montero, J., & Laserna, S. (2017). Influence of effective mixing water in recycled concrete. *Construction and Building Materials*, 132, 343–352.
- Ozbakkaloglu, T., Gholampour, A., & Xie, T. (2017). Mechanical and durability properties of recycled aggregate concrete: Effect of recycled aggregate properties and content. *Journal of Materials in Civil Engineering*, 30(2), 04017275.
- Pedro, D., Brito, J., & Evangelista, L. (2017). Structural concrete with simultaneous incorporation of fine and coarse recycled concrete aggregates: Mechanical, durability and long-term properties. *Construction and Building Materials*, 154, 294–309.
- Pereira, P., Evangelista, L., & Brito, J. (2012a). The effect of superplasticisers on the workability and compressive strength of concrete made with fine recycled concrete aggregates. *Construction and Building Materials*, 28(1), 722–729.
- Pereira, P., Evangelista, L., & Brito, J. (2012b). The effect of superplasticizers on the mechanical performance of concrete made with fine recycled concrete aggregates. *Cement & Concrete Composites*, 34(9), 1044–1052.
- Raphael, J. M. (1984). *Tensile strength of concrete*. *ACI Journal*, 81, 158–165.
- RILEM TC 121. (1994). Specifications for Concrete with Recycled Aggregates. *Materials and Structures*, 27, 557–559.
- Ryou, J., & Lee, Y. S. (2014). Characterization of recycled coarse aggregate (RCA) via a surface coating method. *International Journal of Concrete Structures and Materials*, 8(2), 165–172.
- Ryu, H. S., Kim, D. M., Shin, S. H., Lim, S. M., & Park, W. J. (2018). Evaluation on the surface modification of recycled fine aggregates in aqueous H₂SiF₆ solution. *International Journal of Concrete Structures and Materials*, 12(1), 19.
- Sagoe-Crentsil, K. K., Brown, T., & Taylor, A. H. (2001). Performance of concrete made with commercially produced coarse recycled concrete aggregate. *Cement and Concrete Research*, 31(5), 707–712.
- Santos, S., Silva, P., & Brito, J. (2017). Mechanical performance evaluation of self-compacting concrete with fine and coarse recycled aggregates from the precast industry. *Materials*, 10(8), 904.
- Seo, T. S., & Lee, M. S. (2015). Experimental study on tensile creep of coarse recycled aggregate concrete. *International Journal of Concrete Structures and Materials*, 9(3), 337–343.
- Sim, B. S., & Won, Y. H. (2010). Recycling gravels peeling mortar rotor. *Korea Patent 10-0994728*, 10 Nov. 2010.
- Smith, R., Ferrebee, E., Ouyang, Y., & Roesler, J. (2014). Optimal staging area locations and material recycling strategies for sustainable highway reconstruction. *Computer-Aided Civil and Infrastructure Engineering*, 29(8), 559–571.
- Spanish Code. (2008). *Permanent commission of the concrete*. Madrid: Spanish Ministry of Public Works.
- Tahar, Z. E. A., Ngo, T. T., Kadri, E. H., Bouvet, A., Debieb, F., & Aggoun, S. (2017). Effect of cement and admixture on the utilization of recycled aggregates in concrete. *Construction and Building Materials*, 149, 91–102.
- Tam, V. W. Y., Kotrayothar, D., & Xiao, J. (2015). Long-term deformation behaviour of recycled aggregate concrete. *Construction and Building Materials*, 100, 262–272.
- Wang, C., Xiao, J., & Sun, Z. (2016). Seismic analysis on recycled aggregate concrete frame considering strain rate effect. *International Journal of Concrete Structures and Materials*, 10(3), 307–323.
- Wardeh, G., Ghorbel, E., & Gomart, H. (2015). Mix design and properties of recycled aggregate concretes: Applicability of eurocode 2. *International Journal of Concrete Structures and Materials*, 9(1), 1–20.
- Won, Y. H. (2006). Separating method for remarking building waste. *Korea Patent 10-0633765*, 04 Oct. 2006.
- Won, Y. H., & Sim, B. S. (2009). A cleaning and sorting system for regenerating of building waste. *Korea Patent 10-0896225*, 28 Apr. 2009.
- Xie, T., & Ozbakkaloglu, T. (2016). Behavior of recycled aggregate concrete-filled basalt and carbon FRP tubes. *Construction and Building Materials*, 105, 132–143.
- Yang, K. H., Chung, H. S., & Ashour, A. F. (2008). Influence of type and replacement level of recycled aggregates on concrete properties. *ACI Materials Journal*, 105(3), 289–296.
- Zain, M. F. M., Mahmud, H. B., Ilham, A., & Faizal, M. (2002). Prediction of splitting tensile strength of high-performance concrete. *Cement and Concrete Research*, 32(8), 1251–1258.
- Zega, C. J., & Maio, Á. A. (2011). Use of recycled fine aggregate in concretes with durable requirements. *Waste Management*, 31(11), 2336–2340.
- Zegardlo, B., Szeląg, M., & Ogródnik, P. (2018). Concrete resistant to spalling made with recycled aggregate from sanitary ceramic wastes—The effect of moisture and porosity on destructive processes occurring in fire conditions. *Construction and Building Materials*, 173, 58–68.
- Zhou, C., & Chen, Z. (2017). Mechanical properties of recycled concrete made with different types of coarse aggregate. *Construction and Building Materials*, 134, 497–506.

Publisher's Note

Springer Nature remains neutral with regard to jurisdictional claims in published maps and institutional affiliations.

Submit your manuscript to a SpringerOpen® journal and benefit from:

- Convenient online submission
- Rigorous peer review
- Open access: articles freely available online
- High visibility within the field
- Retaining the copyright to your article

Submit your next manuscript at ► [springeropen.com](https://www.springeropen.com)